Molecular Lithography on Silicon Wafer Guided by Porous, Extended Arrays of Small DNA Tiles

Dake Mao[1], Longfei Liu[1], Cuizheng Zhang[1], Haitao Liu[2], and Chengde Mao[1]*

[1]Purdue University, Department of Chemistry, West Lafayette, IN 47907,USA

[2]University of Pittsburgh, Department of Chemistry, Pittsburgh, PA 15260, USA

Keywords: Molecular Lithography, Nanopatterning, DNA Self-Assembly, DNA Nanostructures

Abstract. Tile-based DNA self-assembly is a cost-effective fabrication method for large-scale nanopatterns. Herein, we report a protocol to directly assemble DNA 2D arrays on silicon wafers and then use the DNA nanostructures as molds to fabricate corresponding nanostructures on the silicon wafers by HF etching. Similar HF etching has been used with robust large DNA origami structures as templates. This work demonstrates that DNA nanostructures assembled from small tiles are sufficiently stable

for this process. The resulting feature size (~ 8.6 nm) approaches the sizes of e-beam lithography. While the reported method is parallel and inexpensive, e-beam lithography is a serial method and is expensive. We expect that this method will be very useful for prepare fine nanopatterns in large areas.

1. Introduction

DNA self-assembly is a promising approach for constructing nanoscale materials with excellent shape control.[1-6] In past decades, a large variety of DNA nanostructures has been achieved. The DNA nanostructure could be designed into complex structures and atomic accuracy, facilitating the application in nanofabrication and manufacturing.[7-11] Recently, DNA nanotechnology has been applied in arranging nanoparticles,[12-16] direct metallization or mineralization on DNA nanostructures,[17-20] and electronic devices.[21-24] Particularly, DNA nanostructure could serve as an etchant-blocking or volatile precursor-protecting mask in surface engineering, transferring the patterns with the same shapes and dimensions as the DNA templates to surfaces.[25-31] In past decades, scientist could prepare DNA 2D crystals directly on the silicon wafer surfaces,[32,33] deposit individual DNA nanostructures on silicon wafer surfaces and permanently transferred the pattern onto the inorganic materials.[26,27,34,35] To expand DNA templates to the massively modification of the entire surface, the DNA pattern should be ordered, position-specific and porous for further masking. Here

we report a general protocol to prepare porous DNA 2D crystals with pre-designed patterns assembled from small DNA tiles on silicon wafers. Then, the DNA crystals could act as the masks in hydrogen fluoride (HF) vapor etching, fabricating the wafers by transferring the periodic 2D patterns to silica surfaces in large areas.

2. Results and Discussion

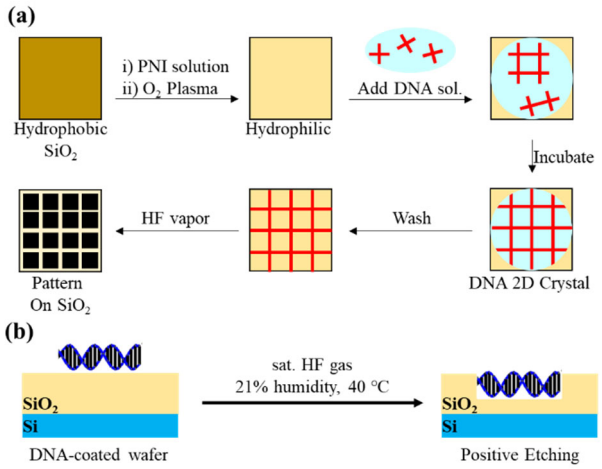

Figure 1. Scheme of the entire protocol. (a) Assembly of DNA 2D array on silicon wafer (containing a native silica layer on top) and DNA-templated nanofabrication. (b) A side view of DNA-masked positive etching of silica by HF gas.

Tile-based DNA self-assembly is a great way for nanofabrication and molecular lithography. Under optimized surface-dependent conditions, DNA tiles can assemble into large, porous, 2D crystalline patterns with different geometries on various substrates. The feature sizes of the DNA tiles are as small as 2-4 nm, which are generally much smaller

than those of DNA origami structures and those from photolithography.[36,37] Moreover, the tile-based DNA self-assembly allows large-scale surface masking with tunable design and low cost. Figure 1 illustrates the overall process. (1) Small piece of silicon wafer was firstly washed with solvent and Piranha solution (PNI solution) to remove dust and organic residues on the surface. (2) After washing, the surface was cleaned by oxygen plasma to generate active hydroxy groups and to introduce hydrophilicity to the surface.[38,39] (3) The top layer of the wafer is a thin layer of SiO_2 (silica). The silicon wafer pieces were incubated with DNA solution, allowing the DNA tiles to assemble into the 2D periodic arrays on the silicon wafer. (4) The surface was dried and desalted, which reserved the 2D arrays alone on the surface. (5) The DNA-masked silicon wafer was etched with hydrogen fluoride (HF) gas and transfer the patterns of DNA arrays as a positive etching (Figure 1b). HF would preferably adsorb near the DNA structures, which are locally condensed moistures in the air. Due to the porous features of the DNA 2D arrays, the chemical vapor etching would differentiate the DNA helixes and cavities. The morphology of nanopatterns were dictated by the assembled DNA nanostructures.

The 2D DNA arrays were assembled on the silicon wafer and observed by AFM according to the reported method.[14,40] In this study, three different 2D arrays were prepared on the silica surface by incubating with three different DNA motifs. To prepare the DNA motif solutions, individual DNA strands were mixed in the TAE/Mg^{2+} buffer at designated concentrations and ratios. The DNA motifs formed upon thermally annealing

from 95 to 22 °C (see the Supporting Information for details). Next, surface-assisted self-assembly was performed on the silicon wafer with assembled DNA motifs and designed metal cation concentrations. Briefly, the annealed DNA motif solution was deposited on the freshly plasma-cleaned silicon wafer and isothermally incubated at 22 °C for 24 hours. After the incubation, the solution was removed, and the wafer was rapidly washed with a solution containing 10 mM Mg^{2+} and 4 mM Ni^{2+} to remove those unbound DNA motifs and salt while maintaining the integrity of the DNA 2D arrays. The dehydrated DNA arrays not only maintained their original structures and provided high spatial resolution during AFM imaging, but also benefited the following vapor-based nanofabrication.

By tuning the concentration of bivalent cation (Mg^{2+}) and monovalent cation (Na^{+}), the surface coverage and homogeneity of DNA 2D arrays could be optimized, leading to the assembly of large single-crystalline arrays. As a bivalent cation, Mg^{2+} could bridge the DNA and surface and increase the binding interaction between DNA backbones and the surface. Generally, low [Mg^{2+}] would weaken the surface-DNA interaction, which decreased the surface coverage and integrity. On opposite, high [Mg^{2+}] endowed high surface deposition rates for DNA and strong binding between DNA motifs and surface, hindering the dynamic 2D array growth and resulting in small polycrystalline domains. Na^{+} is regarded as a completive cation with Mg^{2+} by occupying the DNA backbones, which could weaken and finely tune the DNA-surface interaction strength.[14] Compare

with a recent study using large DNA origami and optimized temperature,[32] the DNA tiles used in this study has relatively small molecular size and weak blunt end inter-motif interaction, which could form single crystal by long-time isothermal incubation, rather than high temperature and avoid multi-layer structures.

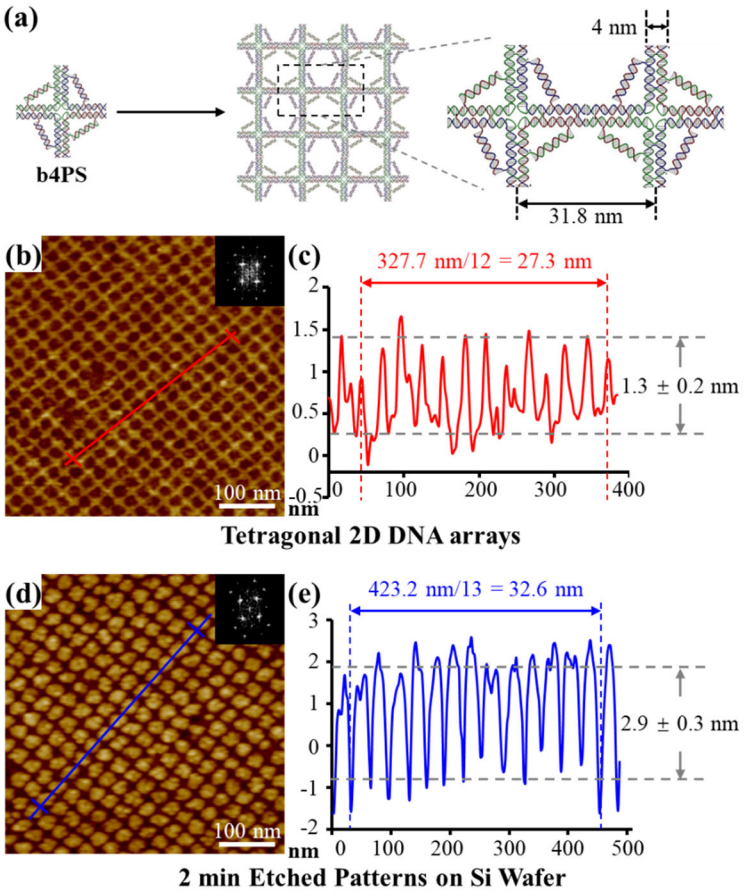

Figure 2. Preparation of tetragonal nanostructures on Silicon wafer. (a) Schematic of b4PS DNA motifs forming tetragonal array and its repeating distance. (b) AFM image of square DNA array on silicon wafer and FFT spots (upper right). (c) Section analysis of (b) (red line). (d) The AFM image of etched b4PS pattern and FFT spots (upper right) (e)

Section analysis of (d) (blue line).

We started our study with the tetragonal arrays assembled from the bridged four-point star DNA motif, b4PS (Figure 2). The rigid b4PS could form large, single-crystalline, tetragonal array on mica surface under the optimized condition, [Mg^{2+}]: 10 mM and [Na^{+}]: 500 mM (Figure 2b). Due to the lower hydroxy group density and hydrophilicity of the silica surfaces,[41] a higher cationic strength was applied on the silicon wafer. At 60 mM Mg^{2+}, the b4PS could cover the surface with relatively large crystal domains (Figure S1b); while at 50 or 70 mM Mg^{2+} the silica surface was either unsaturated or had polycrystals with small domains, respectively (Figure S1a, c). Further addition of 200 mM Na^{+} facilitated growth of the large single-crystalline 2D arrays (Figure S1d). After assembling the single crystalline tetragonal arrays on silica surface, we measured the repeating distance and DNA height by section analysis (Figure 2c, S2a) which were 27.3 nm and 1.3 nm, respectively. These values matched with designs well.

Robust DNA origami nanostructures were applied in molecular lithography as masks for vapor etching or chemical vapor deposition (CVD).[27,42] Herein, we transferred the relatively fragile, DNA 2D arrays onto silicon wafer surface by wet HF vapor etching (Figure 1b). In principle, the HF vapor could react with silica and remove silica solid by generating SiF_4 gas as the following formula.

SiO_2 (solid) + 4 HF (gas) = SiF_4 (gas) + 2 H_2O (gas)

However, Although the reaction is thermodynamically favored, water was commonly added as a catalyst by generating the bifluoride anion (HF_2^-) on the surface to kinetically facilitate the reaction.[39,40]

6 HF (gas) + 3 H_2O (gas) = 3 HF_2 (abs) + 3 H_3O^+ (abs)

3 HF_2 (abs) + 3 H_3O^+ (abs) + SiO_2 (solid) = 2 HF (gas) + SiF_4 (gas) + 5 H_2O (gas)

During the etching, DNA is highly hydrophilic and can absorb water vapor and accumulate HF_2^- around helixes, which results in the positive etching. We carried the lithography process with the evaporation etching equipment. To be specific, a plastic jar was saturated by 48% HF and the humidity was tuned to 21% by saturated potassium acetate solution. Then, DNA 2D array-coated, dehydrated silicon wafers were heated to 40 °C and hung on the open jar and etched for the designated time (Figure S3). After etching, the silicon wafer was thoroughly washed with TAE buffer and then with water to remove HF, salt, and unbound DNAs (Figure S4). The tetragonal array was transferred onto the silicon wafer with the DNA 2D arrays as masks (Figure 2d, S5a). After etching and washing, the morphology of tetragonal DNA 2D array was preserved on the silicon wafer as a positive etching, which removed the silica under the DNAs and formed trenches lower than the surface. Section profiles were plotted along the continuous parallel trenches of tetragonal arrays to determine the repeating distance between two

adjacent trenches, which resulted in an average of 32.5 nm (Fig. 2e, S2b), agreeing well with the theoretical value (31.8 nm). Moreover, the average widths of trenches and islands are 9.1 ± 1.7 nm and 23.2 ± 3.2 nm, respectively (Figure S2b, S4b). The measured trench is wider than the DNA mask width (4 nm, as double duplexes), indicating the HF vapor adsorption is highly guided and fused around the bridge structure in DNA motif design. The etching depth was measured by section analysis of the height difference between the trench bottom and island top, resulting in 2.9 ± 0.3 nm. This narrow distribution of etching depth demonstrates that the DNA-masked, HF vapor etching is uniform and mild.

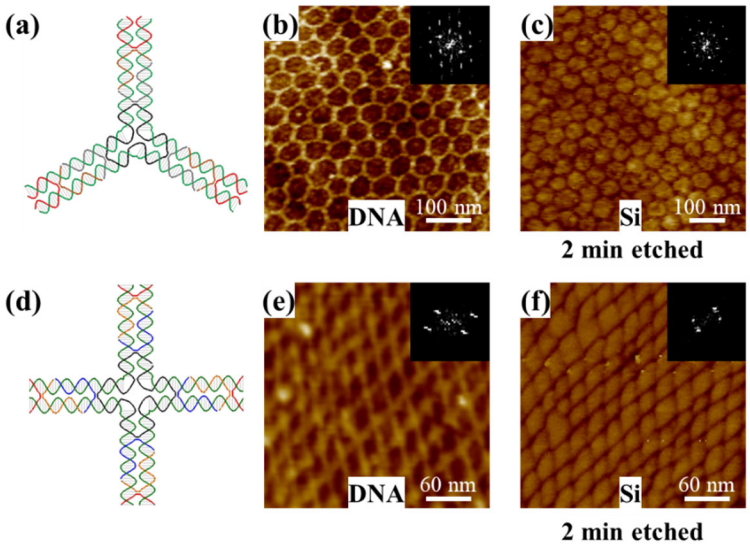

Figure 3. Preparation of nanostructures on Silicon wafer directed by DNA arrays assembled from non-bridged DNA motifs. (a) Scheme of an elongated, three-point-star

motif (e3PS). AFM images of (b) hexagonal arrays assembled from e3PS and (c) the corresponding Si structures. (d) Scheme of a elongated, four-point-star motif (e4PS). AFM images of (e) tetragonal arrays assembled from e4PS and (f) the corresponding Si structures. Each AFM image is accompanied with an corresponding FFT pattern at its upper right corner.

With different DNA motif designs, the honeycomb and rhombus patterns were transferred onto the silicon wafer by HF vapor etching (Figure 3). Correspondingly, the elongated, three-points-star (e3PS) DNA motif (Figure 3a, S6, S7) and elongated, four-points-star (e4PS) DNA motif (Figure 3d, S8, S9) were incubated on the surface with optimal conditions to prepare honeycomb and rhombus patterns, respectively. After surface incubation, the silicon wafer was desalted and dried in the same was as for the tetragonal 2D arrays from the b4PS motif (Figure 3b, 3e). Then, the HF vapor etching process was applied to these two 2D arrays, resulting in the corresponding etched patterns on Si wafer (Figure 3c, 3f). We measured the DNA 2D arrays and the etching patterns by section analysis (Figure S10- S13). The unit repeating distances were well-matched between DNA 2D nanostructures and the nanostructures of silicon wafers. For hexagon patterns, the unit repeating distance was measured as 52.8 nm, agreeing well with the theoretical value 54.3 nm. The depth and trench width for hexagon patterns were 1.3 ± 0.2 nm and 8.6 ± 1.3 nm, respectively; these two values were 1.4 ± 0.2 nm and 6.5 ± 1.0

nm (Figure S14) in rhombus patterns. Presumably, the bridged structure provides higher DNA surface density and stronger structure identity, which results in a more intensive HF condensing and etching rate.

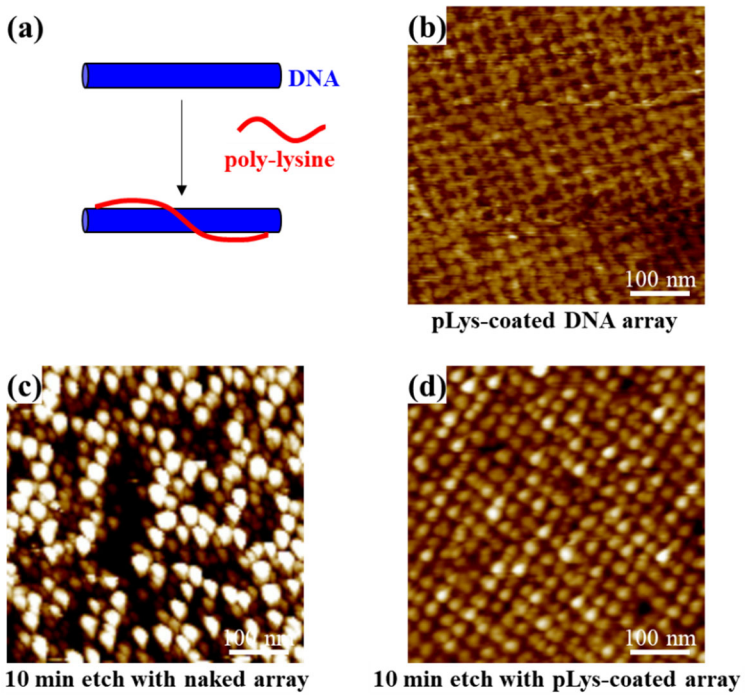

Figure 4. Impact of poly-lysine coating on DNA arrays. (a) Schematic presentation (b) The AFM image of poly-lysine coated DNA b4PS array. The AFM images of 10 min HF etching (c) with naked DNA b4PS arrays and with (d) poly-lysine-coated b4PS arrays.

To improve the structure integrity for dehydrated DNA arrays for the long-time etching, we *in situ* coated the DNA 2D arrays with poly-lysine (pLys) to prepare the

enhanced etching masks. Due to the highly positive charged property, the pLys could wrap on the DNA helixes and thus preserve the original porous 2D array structure under high temperature during vapor etching process (Figure 4a). The DNA array-masked silicon wafer was directly incubated with pLys solution in the presence of Ni^{2+}, then washed to remove excess pLys, and finally desalted as previously mentioned. After pLys treatment, the overall morphology and periodicity of DNA 2D crystals were maintained (Figure 4b, S15) while the dimension of DNA double duplex arms slightly increased (Figure S16), demonstrating the successful coating and dehydration of DNA array. After etching, the pLys-coated DNA arrays could not be completely washed away by TAE buffer and water. So, additional O_2 plasma cleaning was added to ensure that all DNA residues could be removed (Figure S17).

The naked or pLys-coated wafers with DNA tetragonal array were etched under previous protocol with different reaction times for comparison. When the etching time was 2 min, the etching on naked DNA arrays transferred the 2D pattern from DNA arrays to silica surface, while the pLys-coated wafer did not show etching activities. Elongating the time to 5 or 10 min, the etching on naked wafers generated defects and the pattern gradually lose the integrity (Figure 4c, S18a, S18e.). However, the coated wafer could be etched with long reaction time and remained the tetragonal morphology (Figure 4d, S18b, S18f.). We performed the section analysis to evaluate the etching control by the pLys coating (Figure S19, S20). The etching depth for 10 min reaction was increased to 10.9

nm on naked wafer, while the depth could keep at 3.5 nm on pLys coated wafer (Figure S21). The pLys coating significantly enhanced the array stability during etching and lower the etching rate. We reasoned that the pLys coating could have two benefits. First, the coating will decrease the hydrophilicity on the surface by neutralizing charges, condensing less active HF species on the surface and slowing down the etching rate. Second, the entanglement of pLys could mechanically hold DNA strands together and keep the integrity under drying, wet-etching and heating. Although the pLys coating significantly decrease the etching rate, the coating method demonstrated that the DNA mask could be stabilized under harsh vapor etching conditions. Conceivably, artificial nucleic acids, such as PNA or backbone-modified DNA, could assemble to 2D array and guide the etching by the hydrophilicity, but accommodate to more harsh or special conditions.

3. Conclusions

In conclusion, we demonstrated the assembly of porous and periodic 2D crystals with small DNA tiles on silica surfaces by bottom-up strategy. With simple HF vapor etching, the nanostructure of DNA arrays could be reliably transferred into silicon wafers. Compared with previously reported similar studies, this protocol has several attractive features: (i) The DNA nanostructures are *in situ* assembled on silicon wafers and thus

post-assembly transfer is not needed, thus, avoiding the problem of breaking large, single-layer, DNA 2D arrays and rendering the possibility to reach unregular surface of devices. (ii) The DNA nanostructures are assembled from a very small number of unique-sequenced DNA strands in common buffers, instead of hundreds of strands. Thus, this method is cost-effective and can be readily scaled up. (iii) Each edge contains only two duplexes and is only ~ 4 nm wide. Along with the atomic resolution of the self-assembly, that leads to fine features in the final nanostructures in silicon wafer, comparable to those feature sizes from e-beam lithography. (iv) The protocol is friendly to chemists/ biologists as it can be conducted in any chemistry/biology lab and does not require any special facility; thus, provides a simple way for chemists/biologists to fabricate inorganic nanostructures to investigate chemical/biological processes/phenomena at the nanometer scales. In general, our approach provides a mass production method for silicon wafer treatment and surface processing or benefits the microfluid devices design.

4. Experimental Section

4.1. Materials: Silicon wafer with 300 nm oxide layer (Product number: 1432) was purchased by University Wafer. 48% Hydrofluoric Acid is purchased from Mallinckrodt Chemicals. Poly-L-lysine (pLys) (1g/L) is purchased from Ted-Pella. All other chemicals

used in buffer preparation are purchased from Sigma-Aldrich.

Oligonucleotides. DNA sequences have been designed by a computer program "SEQUIN".[1] All oligonucleotides were purchased from IDT Inc., purified by 6% - 20% denaturing PAGE, and their concentrations were quantified by UV-Visible spectroscopy at 260 nm. The DNA sequences and molar ratio of DNA motifs are listed below. The motif b4PS is prepared with literature report.

DNA Strands:

L3: AGGCACCATCGTAGGTTTCTTGCCAGGCACCATCGTAGGTTTCTTGCCAGG CACCATCGTAGGTTTCTTGCC

L4: AGGCACCATCGTAGGTTTTCTTGCCAGGCACCATCGTAGGTTTTCTTGCCAG GCACCATCGTAGGTTTTCTTGCCAGGCACCATCGTAGGTTTTCTTGCC

M3: GACTATGCAACCTGATACCCTTAGTATGTAGCCTGCCTGGCAAGCCTACGA TGGACAATCTATTATGCGATTCGGACACGGTAACGC

M4: GCAACCTGATACCCTTAGTATGTAGCCTGCCTGGCAAGCCTACGATGGACA ATCTATTATGCGATTCGGACACGG

J1: TATCACCGAATCGCATAATAG

J2: ATTGTGGCTACATACTAAGGG

J1b: TATCACCGAATCGCATAATAGCGTCGAACG

J2b: ATTGTGGCTACATACTAAGGGCGTCGAACG

S3: AGGCGTTACCGTGTGGTTGCATAGTCAG

S4: CCGTGTGGTTGC

BB: CATGAAGCTTCATGGTTCGACT

DNA Motifs:

e3PS: L3+M3+J1+J2+S3 (1:3:3:3:3).

e4PS: L4+M4+J1+J2+S4 (1:4:4:4:4).

b4PS: L4+M4+J1b+J2b+S4+BB (1:4:4:4:4:8).

Buffers:

TAE buffer: 40 mM tris base, 2 mM EDTA and 20 mM acetic acid acetate, pH 8.0

TAE/Mg^{2+} buffer: 40 mM tris base, 2 mM EDTA, 20 mM acetic acid and 12.5 mM magnesium acetate, pH 8.0

TAE/xxNa^{+}/xxMg^{2+} (incubation buffer): 40 mM tris base, 20 mM acetic acid, 2 mM EDTA, designated concentration for sodium chloride and magnesium acetate, pH 8.0

TA/Mg^{2+}/Ni^{2+} (post-incubation washing buffer): 40 mM tris base, 20 mM acetic acid, 10 mM magnesium acetate and 2 mM nickel (II) chloride, pH 8.0

Mg^{2+}/Ni^{2+} (desalting buffer): 10 mM magnesium acetate and 4 mM nickel (II) chloride.

4.2. Preparation of individual DNA motifs.

(1) For b4PS motif, mix all ssDNAs (except bridge strands **BB**) at designated stoichiometric molar ratio in TAE/Mg^{2+} solution. Sequentially incubate above solutions: 95 °C for 5 min, 65 °C for 30 min, 50 °C for 30 min, 37 °C for 30 min, and 22 °C for 30 min. [500 nM motif solution (no bridges)]. Add 20 μL of bridge DNA, **BB**, into the annealed solution above and incubate for 24 hours at 22 °C [final 100 μL 400 nM b4PS motif solution (with bridges)].

(2) For e3PS and e4PS, mix all ssDNAs at designated stoichiometric molar ratio in TAE/Mg^{2+} solution. Sequentially incubate above solutions: 95 °C for 5 min, 65 °C for 30 min, 50 °C for 30 min, 37 °C for 30 min, and 22 °C for 30 min [final 100 μL 400 nM e3PS or e4PS motif solution].

4.3. Polyacrylamide gel electrophoresis (PAGE).

Mix 40% acrylamide/bisacrylamide solution (19:1, 5% crosslinker), 10× TAE/Mg^{2+} buffer, and distilled water to prepare 6% native PAGE gel. The running buffer was TAE/Mg^{2+} buffer). Gels were run on a FB-VE10-1 electrophoresis unit (FisherBiotech) at 4 °C (250V, constant voltage) for 5 hours. After electrophoresis, the gels were stained with Stains-all dye (Sigma) and scanned.

4.4. Surface assembly of DNA arrays.

(1) Silica wafer reparation: Silica disc was cut to about 6x6 mm size. Wafers were washed under ultrasound with water, isopropanol and acetone in sequence, then dried by nitrogen gas flow. After fully dried, Wafers were cleaned by Piranha solution (3:1 concentrated H_2SO_4 and 30% H_2O_2) for 25 min at 80 °C. Then, wafers were thoroughly rinsed with water, and wash with washed under ultrasonic with water, isopropanol and acetone in sequence. Finally, wafers were dried by nitrogen gas flow. Before the DNA incubation, the silica wafer was cleaned by O_2 plasma for 10 min.

(2) Mix DNA motif to a final concentration 200 nM DNA in TAE/Na^+/Mg^{2+} (200 mM Na^+, 60 mM Mg^{2+} for b4PS, 60 mM Mg^{2+} for e3PS and e4PS) solution.

(3) Surface assembly: Deposit 10 μL DNA solution onto silicon wafer surface and incubate for 24 hours at 22 °C for array formation.

(4) Array post-treatment: After surface assembly, 25 μL TA/Mg^{2+}/Ni^{2+} buffer was added onto wafer surface and then removed by compressed air. Then 25 μL Mg^{2+}/Ni^{2+} buffer was added wafer mica surface and then thoroughly removed by compressed air. The wafer was directly used in following AFM imaging or HF vapor etching.

4.5. pLys coating of DNA arrays.

After the surface assembly, 25 μL TA/Mg^{2+}/Ni^{2+} buffer was added onto wafer surface and then removed by compressed air. Then, 25 μL TA/Mg^{2+}/Ni^{2+} buffer with 40 μg/mL pLys solution was added onto wafer surface and incubated for 10 min. After pLys incubation,

25 μL TA/Mg^{2+}/Ni^{2+} buffer was added onto wafer surface and then removed by compressed air. Then 25 μL Mg^{2+}/Ni^{2+} buffer was added onto wafer surface and then thoroughly removed by compressed air. The wafer was directly used in following AFM imaging or HF vapor etching.

4.6. AFM images

AFM images were captured by MultiMode 8 (Bruker or Veeco) using tapping mode with HQ:NSC19/Al BS probes (MikroMasch). For AFM parameters: the Z limit is 3.6 μm, integral gain is 0.7, proportional gain is 0.5, driving amplitude is 1000 mV, the set point is varied from 100-500 mV. All experiments were carried out at 22 °C.

4.7. HF vapor etching

(1) Etching chamber preparation: 3 mL 48% HF and 20 mL saturated potassium acetate solution (with about 10 g salt solid) in a 32 oz plastic jar, incubate for at least 24 hours. A 1.5x1.5 cm small hole was on the top of the jar.

(2) Etching: The DNA-masked silica wafer was reversely sticked on a metal water tank, in which 1 L 40 °C water was filled. The tank was placed on the jar and wafers were aligned above the hole. Thus, the HF vapor with 21 % humidity could contact wafer. Wafer was etched for designated time.

(3) Post-treatment after etching: The tank was flipped to make wafers face up. The wafers

were immediately blow by compressed air for 5 s. Then, the wafer was put in 1 mL TAE solution for 10 min, following with putting in water for 10 min (TAE-water wash). Finally, the wafer was dried by compressed air and imaged by AFM. For PLL coating sample, the wafer was additionally cleaned by cleaned by O_2 plasma for 10 min before AFM imaging.

Supporting Information.

Additional experimental data on characterization of DNA structures and nanostructures on silicon wafer.

Author Information

Corresponding Author

Chengde Mao – Purdue University, Department of Chemistry, West Lafayette, Indiana 47907, USA. https://orcid.org/0000-0001-7516-8666; Email: mao@purdue.edu

Authors

Dake Mao – Purdue University, Department of Chemistry, West Lafayette, Indiana 47907, USA. https://orcid.org/0000-0002-6824-2159

Longfei Liu – Purdue University, Department of Chemistry, West Lafayette, Indiana 47907, USA. http://orcid.org/0000-0002-5760-2964

Cuizheng Zhang – Purdue University, Department of Chemistry, West Lafayette, Indiana 47907, USA. http://orcid.org/0000-0003-3342-7003

Haitao Liu – University of Pittsburgh, Department of Chemistry, Pittsburgh, Pennsylvania 15206, USA. http://orcid.org/0000-0003-3628-5688

Notes

The authors declare no competing financial interest.

ACKNOWLEDGEMENT

We thank NSF (CCF2107393, CMMI2025187) for financial support to this work.

REFERENCE

1. Matthew R. Jones, Nadrian C. Seeman and Chad A. Mirkin. Programmable materials and the nature of the DNA bond. *Science.* **347**, 1260901 (2015).

2. Constantine G. Evans and Erik Winfree. Physical principles for DNA tile self-assembly. *Chem. Soc. Rev.* **46**, 3808–3829 (2017).

3. Andre V. Pinheiro, Dongran Han, William M. Shih and Hao Yan. Challenges and opportunities for structural DNA nanotechnology. *Nat. Nanotechnol.* **6**, 763–772 (2011).

4. Jiang Li, Alexander A. Green, Hao Yan and Chunhai Fan. Engineering nucleic acid structures for programmable molecular circuitry and intracellular biocomputation. *Nat. Chem.* **9**, 1056–1067 (2017).

5. Nadrian C. Seeman and Hanadi F. Sleiman. DNA nanotechnology. *Nat. Rev. Mater.* **3**, 17068 (2017).

6. Qinqin Hu, Hua Li, Lihua Wang, Hongzhou Gu and Chunhai Fan. DNA nanotechnology-enabled drug delivery systems. *Chem. Rev.* **119**, 6459–6506 (2019).

7. Zhenbo Peng and Haitao Liu. Bottom-up nanofabrication using DNA nanostructures. *Chem. Mater.* **28**, 1012–1021 (2016).

8. Liwei Hui, Qinmei Zhang, Wei Deng and Haitao Liu. DNA-based nanofabrication: pathway to applications in surface engineering. *Small*. 1805428 **15** (2019).

9. Yan Zhao, Xinpei Dai, Fei Wang, Xueli Zhang, Chunhai Fan and Xiaoguo Liu. Nanofabrication based on DNA nanotechnology. *Nano Today*. **26**, 123–148 (2019).

10. Hanying Li, Joshua D. Carter and Thomas H. LaBean. Nanofabrication by DNA self-assembly. *Mater. Today*. **12**, 24–32 (2009).

11. Zhilei Ge, Hongzhou Gu, Qian Li and Chunhai Fan. Concept and development of framework nucleic acids. *J. Am. Chem. Soc.* **140**, 17808–17819 (2018).

12. Anton Kuzyk, Robert Schreiber, Zhiyuan Fan, Günther Pardatscher, Eva Maria Roller, Alexander Högele, Friedrich C. Simmel, Alexander O. Govorov and Tim Liedl. DNA-based self-assembly of chiral plasmonic nanostructures with tailored optical response. *Nature*. **483**, 311–314 (2012).

13. Ye Tian, Tong Wang, Wenyan Liu, Huolin L. Xin, Huilin Li, Yonggang Ke, William M. Shih and Oleg Gang. Prescribed nanoparticle cluster architectures and low-dimensional arrays built using octahedral DNA origami frames. *Nat. Nanotechnol.* **10**, 637–644 (2015).

14. Longfei Liu, Mengxi Zheng, Zhe Li, Qian Li and Chengde Mao. Patterning nanoparticles with DNA molds. *ACS Appl. Mater. Interfaces*. **11**, 13853–13858 (2019).

15. Linjie Guo, Yueyue Zhang, Yue Wang, Mo Xie, Jiangbing Dai, Zhibei Qu, Mo Zhou, Shuting Cao, Jiye Shi, Lihua Wang, Xiaolei Zuo, Chunhai Fan and Jiang Li. Directing multivalent aptamer-receptor binding on the cell surface with programmable atom-like nanoparticles. *Angew. Chem. Int. Ed.* **61** e202117168 (2022).

16. Yu He, Tao Ye, Alexander E Ribbe and Chengde Mao. DNA-templated fabrication of two-dimensional metallic nanostructures by thermal evaporation coating. *J. Am. Chem. Soc.* **133**, 1742–1744 (2011).

17. Xiaoguo Liu, Xinxin Jing, Pi Liu, Muchen Pan, Zhuo Liu, Xinpei Dai, Jianping Lin, Qian Li, Fei Wang, Sichun Yang, Lihua Wang and Chunhai Fan. DNA framework-encoded mineralization of calcium phosphate. *Chem*. **6**, 472–485 (2020).

18. Xiaoguo Liu, Fei Zhang, Xinxin Jing, Muchen Pan, Pi Liu, Wei Li, Bowen Zhu, Jiang Li, Hong Chen, Lihua Wang, Jianping Lin, Yan Liu, Dongyuan Zhao, Hao Yan and Chunhai Fan. Complex silica composite nanomaterials templated with DNA origami. *Nature*. **559**, 593–598 (2018).

19. Wei Sun, Etienne Boulais, Yera Hakobyan, Wei Li Wang, Amy Guan, Mark Bathe and Peng Yin. Casting inorganic structures with DNA molds. *Science.* **346** 1258361 (2014).

20. Xinpei Dai, Xiaoliang Chen, Xinxin Jing, Yinan Zhang, Muchen Pan, Mingqiang Li, Qian Li, Pi Liu, Chunhai Fan and Xiaoguo Liu. DNA rigami-encoded integration of heterostructures. *Angew. Chem. Int. Ed.* **61** e202114190 (2022).

21. Mengyu Zhao, Yahong Chen, Kexin Wang, Zhaoxuan Zhang, Jason K. Streit, Jeffrey A. Fagan, Jianshi Tang, Ming Zheng, Chaoyong Yang, Zhi Zhu and Wei Sun. DNA-directed nanofabrication of high-performance carbon nanotube field-effect transistors. *Science.* **368**, 878–881 (2020).

22. Liwei Hui, Ruobing Bai and Haitao Liu. DNA-based nanofabrication for nanoelectronics. *Adv. Funct. Mater.* **32** 2112331 (2022).

23. Xinpei Dai, Qian Li, Ali Aldalbahi, Lihua Wang, Chunhai Fan and Xiaoguo Liu. DNA-based fabrication for nanoelectronics. *Nano Lett.* **20**, 5604–5615 (2020).

24. Basu R. Aryal, Dulashani R. Ranasinghe, Tyler R. Westover, Diana G. Calvopiña, Robert C. Davis, John N. Harb and Adam T. Woolley. DNA origami mediated electrically connected metal—semiconductor junctions. *Nano Res.* **13**, 1419–1426 (2020).

25. Zhong Jin, Wei Sun, Yonggang Ke, Chih Jen Shih, Geraldine L.C. Paulus, Qing Hua Wang, Bin Mu, Peng Yin and Michael S. Strano. Metallized DNA nanolithography for encoding and transferring spatial information for graphene patterning. *Nat. Commun.* **4** 1663 (2013).

26. Sumedh P. Surwade, Feng Zhou, Bryan Wei, Wei Sun, Anna Powell, Christina O'Donnell, Peng Yin and Haitao Liu. Nanoscale growth and patterning of inorganic oxides using DNA nanostructure templates. *J. Am. Chem. Soc.* **135**, 6778–6781 (2013).

27. Sumedh P. Surwade, Shichao Zhao and Haitao Liu. Molecular lithography through DNA-mediated etching and masking of SiO_2. *J. Am. Chem. Soc.* **133**, 11868–11871 (2011).

28. Zhaoxiang Deng and Chengde Mao. Molecular lithography with DNA nanostructures. *Angew. Chem. Int. Ed.* **43**, 4068–4070 (2004).

29. Cheikh Tidiane Diagne, Christophe Brun, Didier Gasparutto, Xavier Baillin and Raluca Tiron. DNA origami mask for sub-ten-nanometer lithography. *ACS Nano*. **10**, 6458–6463 (2016).

30. Boxuan Shen, Veikko Linko, Kosti Tapio, Siim Pikker, Tibebe Lemma, Ashwin Gopinath, Kurt V. Gothelf, Mauri A. Kostiainen and J. Jussi Toppari. Plasmonic nanostructures through DNA-assisted lithography. *Sci. Adv.* **4**, eaap8978 (2018).

31. Jie Shen, Wei Sun, Di Liu, Thomas Schaus and Peng Yin. Three-dimensional nanolithography guided by DNA modular epitaxy. *Nat. Mater.* **20**, 683–690 (2021).

32. Kosti Tapio, Charlotte Kielar, Johannes M. Parikka, Adrian Keller, Heini Järvinen, Karim Fahmy and J. Jussi Toppari. Large-scale formation of DNA origami lattice on silicon. *Chem. Mater.* **5**, 1961-1971 (2023).

33. Junwye Lee, Sunho Kim, Junghoon Kim, Chang Won Lee, Yonghan Roh and Sung Ha Park. Coverage control of DNA crystals grown by silica assistance. *Angew. Chem. Int. Ed.* **50**, 9145–9149 (2011).

34. Feng Zhou, Brian Michael, Sumedh P. Surwade, Karen B. Ricardo, Shichao Zhao and Haitao Liu. Mechanistic study of the nanoscale negative-tone pattern transfer from DNA nanostructures to SiO_2. *Chem. Mater.* **27**, 1692–1697 (2015).

35. Guillaume Thomas, Cheikh Tidiane Diagne, Xavier Baillin, Thierry Chevolleau, Thomas Charvolin and Raluca Tiron. DNA Origami for Silicon Patterning. *ACS Appl. Mater. Inter.* **12**, 36799-36809 (2020)

36. Alberto Pirati, Rudy Peeters, Daniel Smith, Sjoerd Lok, Martijn van Noordenburg, Roderik van Es, Eric Verhoeven, Henk Meijer, Arthur Minnaert, Jan-Willem van der Horst, Hans Meiling, Joerg Mallmann, Christian Wagner, Judon Stoeldraijer, Geert Fisser, Jo Finders, Carmen Zoldesi, Uwe Stamm, Herman Boom, David Brandt, Daniel Brown, Igor Fomenkov and Michael Purvis. EUV lithography performance for manufacturing: status and outlook. *Extrem. Ultrav. Lithogr. VII*. **9776**, 97760A (2016).

37. Hong Xu, Vasiliki Kosma, Emmanuel Giannelis, Christopher K. Ober and Kazunori Sakai. EUV photolithography: resist progress and challenges. *Extrem. Ultrav. Lithogr. IX*. **10583**, 15–27 (2018).

38. Ashwin Gopinath, Evan Miyazono, Andrei Faraon and Paul W.K. Rothemund. Engineering and mapping nanocavity emission via precision placement of DNA origami. *Nature*. **535**, 401–405 (2016).

39. Ashwin Gopinath, Chris Thachuk, Anya Mitskovets, Harry A. Atwater, David Kirkpatrick and Paul W.K. Rothemund. Absolute and arbitrary orientation of single-molecule shapes. *Science.* **371** eabd6179 (2021).

40. Longfei Liu, Yulin Li, Yong Wang, Jianwei Zheng and Chengde Mao. Regulating DNA self-assembly by DNA–surface interactions. *ChemBioChem*. **18**, 2404–2407 (2017).

41. Yong Il Lee, Kyung Ho Park, Jonghyun Lee, Chun Su Lee, Hyung Joun Yoo, Chang Jin Kim and Yong San Yoon. Dry release for surface micromachining with HF vapor-phase etching. *J. Microelectromech. Syst.* **6**, 226–233 (1997).

42. Won Ick Jang, Chang Auck Choi, Myung Lae Lee, Chi Hoon Jun and Youn Tae Kim. Fabrication of MEMS devices by using anhydrous HF gas-phase etching with alcoholic vapor. *J. Micromech. Microeng.* **12**, 297–306 (2002).

TOC

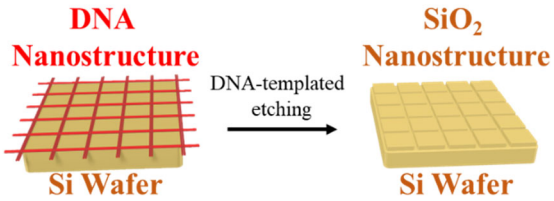
DNA
Nanostructure
Si Wafer
DNA-templated
etching
SiO_2
Nanostructure
Si Wafer